

Dielectric properties and ac conductivities of $\text{Bi}_{1-x}\text{Sm}_x\text{FeO}_3$ ceramics

S. A. Sadykov^a, S. N. Kallaev^{a,b}, N. M.-R. Alikhanov^{a,b}, K. Bormanis^c, and A. Kalvane^c

^aPhysical Department, Dagestan State University, Makhachkala, Russia; ^bDagestan Science Centre, Institute of Physics, RAS, Makhachkala, Russia; ^cInstitute of Solid State Physics, University of Latvia, Riga, Latvia

ABSTRACT

Dielectric permittivity, dielectric losses and ac-conductivity of polycrystalline $\text{Bi}_{1-x}\text{Sm}_x\text{FeO}_3$ ($x=0; 0.05; 0.1; 0.15; 0.2$) are measured in the frequency range 1 kHz–10 MHz and in the temperature range 25–600 °C. Anomalies have been observed at the 200 °C, 300 °C and at the Néel temperature. It has been demonstrated that doping with Sm has enhanced the dielectric properties and increased conduction in the frequency region <1 MHz. At high frequency (>1 MHz) and at a certain temperature T_m , depending on the composition $\text{Bi}_{1-x}\text{Sm}_x\text{FeO}_3$, the conductivity reaches a maximum. The results are discussed with reference to the model of correlated barrier hopping.

ARTICLE HISTORY

Received 2 October 2018

Accepted 8 February 2019

KEYWORDS

BiFeO_3 ceramics; dielectric properties; conductivity

1. Introduction

Multiferroics attract a great deal of researchers' attention due to simultaneous coexistence of ferroelectric and magnetic properties in one phase. One of the most promising multiferroics is BiFeO_3 (BFO), chiefly, due to the high temperatures of the antiferromagnetic ($T_N = 370^\circ\text{C}$) and ferroelectric ordering $T_C = 830^\circ\text{C}$ [1, 2]. The unique properties of BFO and BFO-based materials, render them suitable for use in various magnetoelectric devices, spintronics, sensor technology, and magnetic memory. However, the functionality of BFO is limited by the presence of impurity phases and various kinds of structure defects that arise when it is fabricated and generate dielectric losses and high leakage currents. Low resistivity as well as high leakage current result in deterioration of its ferroelectric properties. Most authors attribute a deterioration in the electrical properties of BFO to non-stoichiometric oxygen deficiency [3, 4], as well as the presence of concomitant phases [5].

2. Experiments

This study investigates the behavior of nanopowder and ceramic samples of $\text{Bi}_{1-x}\text{Sm}_x\text{FeO}_3$ (BSFO- x) ($x=0-0.2$), synthesized by burning nitrate of organic precursors. The initial reagents $\text{Bi}(\text{NO}_3)_3$, $\text{Fe}(\text{NO}_3)_3$ and $\text{Sm}(\text{NO}_3)_3$ (purity > 98%), taken in

the stoichiometric molar ratio, were dissolved in distilled water. Glycine was added to the mixture in the specified proportion. The solution was stirred and let to evaporate and, a nanopowder containing BFO nanocrystals was synthesized as the result of the flare effect.

Diffraction analysis and nanopowder dispersion estimation were carried out on a PANalytical Empyrean series 2 diffractometer using Cu-K α radiation ($\lambda = 1.54056$ Å). The capacitance (C) and conductance (G) were measured on LCR-78110G (Good Will Instrument Co) meter in the frequency (1 kHz–10 MHz) and temperature (25–600 °C) range. To investigate the dielectric constant, the powders Bi $_{1-x}$ Sm $_x$ FeO $_3$ ($x = 0-0.2$) were pressed in the cylindrical form of a flat capacitor with a thickness of ~ 1 mm and a diameter of ~ 6 mm with contacts from a silver-containing paste.

3. Results and discussion

The XRD patterns of BSFO samples are shown in Figure 1. It was found that BSFO-5 as well as BFO crystallizes in rhombohedral structure with R3c space group. XRD analysis of the composition BSFO-10 indicates the presence of a new orthorhombic (space group: Pbam) phase. With 15% bismuth substitution, the crystal structure is completely transformed from rhombohedral to orthorhombic phase.

The temperature dependences of ϵ' and $\tan\delta$, measured at a frequency of 1 kHz for all compositions, are shown in Figure 2. The intense temperature growth of the real part ϵ' begins above 200 °C, reaches a local maximum at ~ 230 °C, and its maximum value $\epsilon'(T)$ is reached at ~ 300 °C. The third peak, $\epsilon'(T)$, is found near ~ 350 °C, in the vicinity of the Neel temperature T_N . We note that the dependences of $\epsilon'(T)$ and $\tan\delta(T)$ for all investigated samples follow the nearly identical pattern. The anomaly in the region ~ 240 °C is clearly evident in compositions with a higher samarium concentration (BSFO-15, BSFO-20). Moreover, the maximum of the values of $\epsilon'(T)$ for these compounds differs by almost an order of magnitude from the initial composition of the

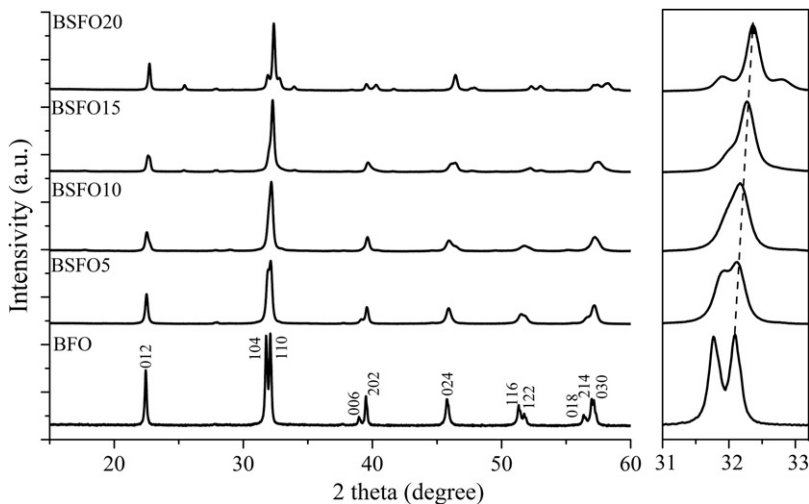


Figure 1. XRD patterns for Bi $_{1-x}$ Sm $_x$ FeO $_3$ samples.

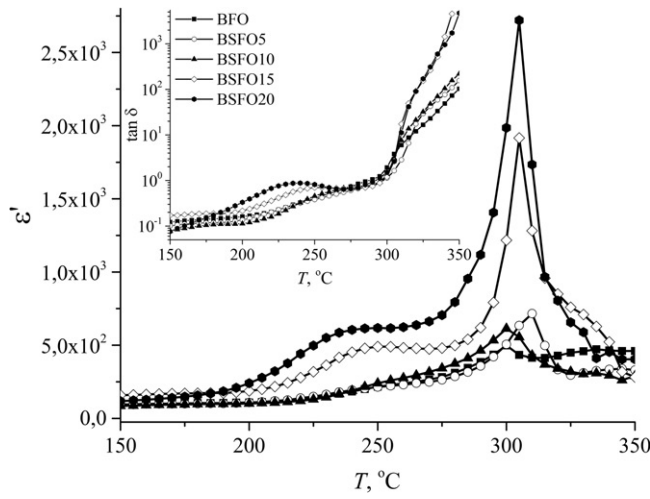


Figure 2. Thermal dependence $\epsilon'(T)$ and $\tan\delta$ at 1 kHz for $\text{Bi}_{1-x}\text{Sm}_x\text{FeO}_3$.

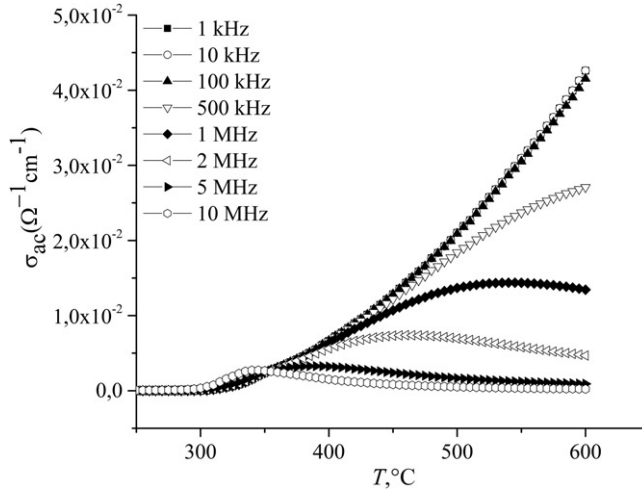


Figure 3. Thermal dependence $\sigma_{ac}(T)$ for BSFO-15.

BSFO. Compositions with a high content of samarium demonstrate a more intensive growth of $\tan\delta(T)$ and relatively high values near T_N (inset, [Figure 2](#)).

The temperature variations ϵ' and $\tan\delta$ of multiferroics are usually attributed to the conductivity of the sample due to polarization phenomena. [Figure 3](#) shows the temperature dependence of σ_{ac} of the composition of BSFO-15. The conductivity of σ_{ac} exhibits strong frequency dispersion. At low frequencies (<1 MHz) and temperatures above 300°C , the conductivity rises to 600°C . This character $\sigma_{ac}(T)$ will also manifest in other compositions ([Figure 4a](#)). In the high-temperature region, at frequencies >1 MHz, the character of the dependence $\sigma_{ac}(T)$ varies radically: at a certain temperature T_m , the conductivity passes through a maximum, and with increasing frequency T_m shifts toward low temperatures and decreases in magnitude ([Figure 4a](#) (insert)). In turn, the

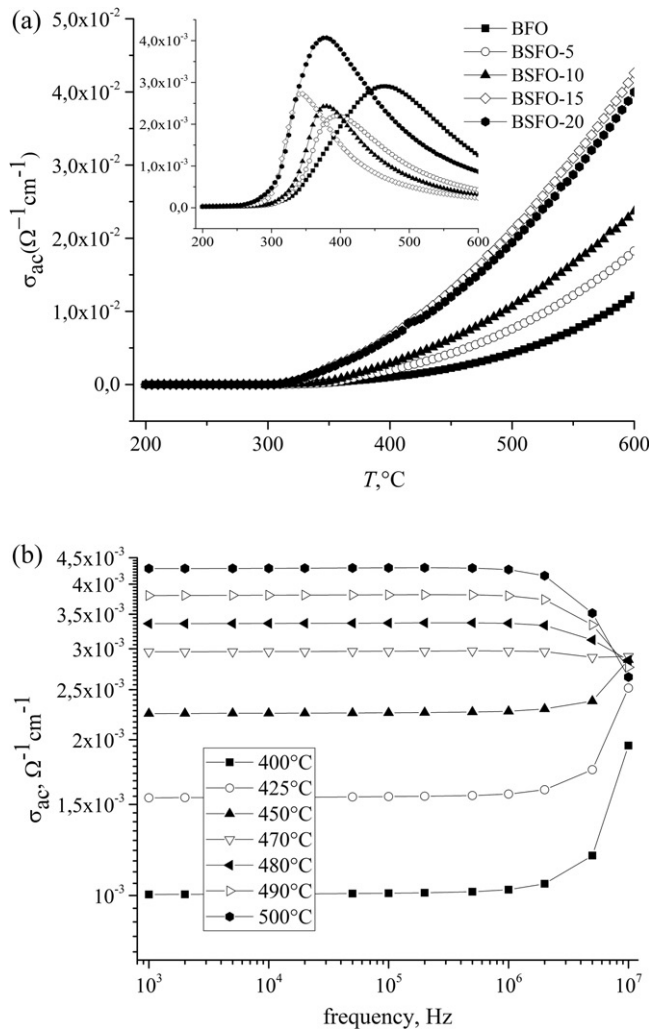


Figure 4. (a) Temperature dependences of the conductivity σ_{ac} of Bi_{1-x}Sm_xFeO₃ at 1kHz and 10MHz (insert); (b) frequency dependence of σ_{ac} of BFO.

temperature position of T_m also depends on the concentration of Sm in the structure of the samples. Figure 4a (insert) shows that at the frequency of 10 MHz, the offset ΔT_m for BSFO-15 relative to BFO reaches more than 100 $^{\circ}\text{C}$. In addition, above the critical temperature T_m , the rate of decrease in conductivity of samples with a high Sm content is higher than that of BFO. As a result, the conductivity of substituted BSFO samples is significantly lower than that of BFO. Figure 4(b) shows the dependence of $\sigma_{ac}(\omega)$ for BFO, from which it follows that above the temperature T_m , the nature of the frequency dependence of the conductivity changes.

The frequency dependence of σ_{ac} in multiferroics can be explained, recalling the electron hopping conductivity model, which assumes electron hopping between localized states of Fe²⁺ and Fe³⁺ ions in grains and displacement of oxygen vacancies at their boundaries [6].

The low-frequency conductivity is identified with the dc conductivity (σ_{dc}). At frequencies >100 kHz conductivity behavior can be interpreted in the context of frame of the model of correlated barrier hopping (CBH) of charge carriers [7]. The anomalous behavior of high-frequency conductivity (>1 MHz) in the high-temperature region can be explained in terms of the carrier-charge transfer electron transfer model, if we take into account the relationship between the hopping frequency ω_h and the frequency of the applied alternating field ω . Under the condition $\omega > \omega_h$, the charge carriers do not have sufficient time to follow the electric field. An increase in the ratio of the number of unsuccessful jumps charge carriers to the number of successful jumps leads to an increase in the dispersion of conductivity in this frequency range [8].

4. Conclusion

X-ray diffraction data revealed formation in the composition BSFO with $x=0.1$ along with the rhombohedral R3c phase of the orthorhombic Pbam phase. The structural phase transition from the polar R3c phase to the non-polar Pbam phase with an increase in the Sm concentration gives rise to a dielectric constant. In the high-frequency region (>1 MHz), at a certain temperature T_m , the conductivity passes through a maximum, and as the frequency T_m increases, the stronger fraction shifts towards the lower temperatures. The conductivity of doped BSFO samples is higher than that of the original BFO.

References

1. W. Eerenstein, N. D. Mathur, and J. F. Scott, Multiferroic and magnetoelectric materials, *Nature*. **442** (7104), 759 (2006). DOI: [10.1038/nature05023](https://doi.org/10.1038/nature05023).
2. G. Catalan, and J. F. Scott, Physics and applications of bismuth ferrite, *Adv. Mater.* **21** (24), 2463 (2009). DOI: [10.1002/adma.200802849](https://doi.org/10.1002/adma.200802849).
3. T. D. Rao, and S. Asthana, Evidence of improved ferroelectric phase stabilization in Nd and Sc co-substituted BiFeO₃. *J. Appl. Phys.* **116**, 164102 (2014). DOI: [10.1063/1.4898805](https://doi.org/10.1063/1.4898805).
4. E. Palaimiene *et al.*, Dielectric investigations of polycrystalline samarium bismuth ferrite ceramic. *Appl. Phys. Lett.* **106** (1), 012906 (2015).
5. A. Lahmar *et al.*, Off-stoichiometry effects on BiFeO₃ thin films. *Solid State Ionics*. **202** (1), 1 (2011). DOI: [10.1016/j.ssi.2011.03.017](https://doi.org/10.1016/j.ssi.2011.03.017).
6. B. Deka, S. Ravi, and D. Pamu, Evolution of structural transition, grain growth inhibition and collinear antiferromagnetism in (Bi_{1-x}Sm_x)FeO₃ ($x = 0$ to 0.3) and their effects on dielectric and magnetic properties. *Ceram. Int.* **43** (18), 16580 (2017). DOI: [10.1016/j.ceramint.2017.09.046](https://doi.org/10.1016/j.ceramint.2017.09.046).
7. S. R. Elliott, A.c. conduction in amorphous chalcogenide and pnictide semiconductors. *Adv. Phys.* **36** (2), 135 (1987). DOI: [10.1080/00018738700101971](https://doi.org/10.1080/00018738700101971).
8. S. A. Sadykov *et al.*, AC conductivity of BiFeO₃ ceramics obtained by spark plasma sintering of nanopowder. *Phys. Solid State*. **59** (9), 1771 (2017).